


## Article

# A Fiducial-Aided Reconfigurable Artefact for the Estimation of Volumetric Errors of Multi-Axis Ultra-Precision Machine Tools

Shixiang Wang <sup>1,2</sup>, Chifai Cheung <sup>2,\*</sup>  and Lingbao Kong <sup>1</sup> 

<sup>1</sup> Shanghai Engineering Research Center of Ultra-Precision Optical Manufacturing, School of Information Science and Technology, Fudan University, Shanghai 200433, China; wangsx@fudan.edu.cn (S.W.); lkong@fudan.edu.cn (L.K.)

<sup>2</sup> State Key Laboratory of Ultra-Precision Machining Technology, Department of Industrial and Systems Engineering, The Hong Kong Polytechnic University, Hung Hom, Kowloon, Hong Kong

\* Correspondence: benny.cheung@polyu.edu.hk

**Abstract:** In this paper, a fiducial-aided reconfigurable artefact is presented for estimating volumetric errors of multi-axis machine tools. The artefact makes use of an adjustable number of standard balls as fiducials to build a 3D artefact which has been calibrated on a coordinate measuring machine (CMM). This 3D artefact demonstrates its reconfigurability in its number of fiducials and their locations according to the characteristics of workpieces and machine tools. The developed kinematics of the machine tool were employed to identify the volumetric errors occupied by the workpiece in the working space by comparing the information acquired by on-machine metrology with that acquired by the CMM. Experimental studies are conducted on a five-axis ultra-precision machine tool. A developed 3D artefact composed of five standard spheres is measured by the integrated on-machine measurement system. Factors including the gravity effect and measurement repeatability are also examined in order to optimize the geometry of the artefact. The results show that the developed 3D artefact is able to provide information about the working space occupied by the workpiece.

**Keywords:** ultra-precision machining; on-machine laser scanner; reconfigurable artefact; fiducial; volumetric errors; machine tools



**Citation:** Wang, S.; Cheung, C.; Kong, L. A Fiducial-Aided Reconfigurable Artefact for the Estimation of Volumetric Errors of Multi-Axis Ultra-Precision Machine Tools. *Appl. Sci.* **2022**, *12*, 1824. <https://doi.org/10.3390/app12041824>

Academic Editors: Zhongchen Cao, Mark J. Jackson, Haitao Liu and Mingyu Liu

Received: 4 December 2021

Accepted: 8 February 2022

Published: 10 February 2022

**Publisher's Note:** MDPI stays neutral with regard to jurisdictional claims in published maps and institutional affiliations.



**Copyright:** © 2022 by the authors. Licensee MDPI, Basel, Switzerland. This article is an open access article distributed under the terms and conditions of the Creative Commons Attribution (CC BY) license (<https://creativecommons.org/licenses/by/4.0/>).

## 1. Introduction

Multi-axis machine tools are key equipment in advanced industries for manufacturing complex freeform components, especially in the fields of ultra-precision diamond turning and polishing. The accuracy of the workpiece is significantly influenced by the geometric error of these machines. These errors have integrated effects in the manufacture of the products. The modeling and measurement of these volumetric errors are of prime importance in high precision machine tools. As a result, it is recommended to regularly verify the accuracy of machine tools [1,2]. In order to improve the machining accuracy and efficiency, many approaches have been reported to measure and compensate for the geometric error [2–4].

In the development of the error model, the homogeneous transformation matrix (HTM) [5] method is commonly used. This method makes use of all the motion matrix based on rigid body kinematics to establish the relationship between the tool tip and the workpiece. Although it is easy to understand, the calculation may be difficult and time-consuming. In order to improve the efficiency of the calculation, other corresponding approaches have also been proposed such as Denavit–Hartenberg (D-H) transformation matrix [6], the screw theory [7,8] and the differentiable manifold-based method [4]. For the identification of the geometric errors, the laser interferometer [9,10] is the most popular measuring device to directly measure the error of the translational axes due to its high accuracy. However, this method is time-consuming due to the repeated process of adjusting the laser path before every measuring task. A laser ball bar and tracker [11–13] are also

used to measure the volumetric error in an indirect way. These approaches can provide reach information for the evaluation of machine performance. However, it is interesting to note that they all need to incorporate special instruments into the machine, thus requiring specialized personnel and leading to low efficiency. To address this problem, an artefact is employed to improve the effectiveness. A uncalibrated master ball artefact was proposed by [14], which claimed that the new artefact design could provide the volumetric distortion of the entire working space. However, this method may be limited by the low accuracy of the on-machine measurement system.

Bringmann et al. [15] developed a 2D ball plate which can form a 3D working volume by moving the plate in a three-axis machine tool. Mayer [16] probed a scale enriched reconfigurable uncalibrated master ball artefact with the on-machine measuring system to separate the setup errors from the volumetric error of a five-axis machine tool. In addition, a ball dome artefact consisting of 25 precision balls was also fabricated [17] to check the performance of a multi-axis machine tool. These studies are performed on a high-precision machine tool in order to check all of the whole volumetric errors of the machine. Most of these methods can only achieve accuracy at several micrometers and they are focused on all the volumetric errors of the machine tool, which is not true of the precision manufacturing of freeform optics in a specified workspace of the ultra-precision machine tool.

As a result, a reconfigurable fiducial-aided 3D artefact which has the advantage of taking the characteristics of the machined workpiece into consideration is purposely designed in this study. Uncertainties including the gravity effect and measurement repeatability are examined to optimize the reconfigurable artefact. Hence, the HTM is employed to generate the kinematics model of a five-axis machine tool. An integrated on-machine measuring system is developed to evaluate the working volumetric errors in the machining process.

## 2. Research Methodology

### 2.1. Reconfigurable Fiducial-Aided Positioning System Design

The fiducial-aided calibrating and positioning artefact is not only designed to explore its capacity for positioning freeform surfaces in the manufacturing cycle, including manufacture, measurement and evaluation, but also identify the errors (i.e., geometric volumetric errors) of the corresponding machine tool. As a result, the designed reconfigurable fiducial-aided model should suit the machining and measuring conditions well, such as the working space, machine kinematics, tool collision and clamping. Standard balls are good fiducials because their positions can be easily acquired by many touch probe-based on-machine CNC measurement instruments.

The basic idea is the design of a workpiece fixture with a cuboid or cylindrical shape which is capable of being clamped easily in the machines. The ball bars are then assembled at the tips of rods which are mounted surrounding the workpiece with different heights so that a 3D space enveloping the machining work volume is established. The idea behind the variable heights of the balls is that richer information about the working space of the machines can be gathered as well as achieving additional geometric constraints. It is clear that the reconfiguration ability, depending on the working environment (i.e., machine tools, workpiece), is the most important feature of the new fiducial-aided design. It is noted that this characteristic provides the possibility of obtaining specific information in the desired areas. It has the ability to overcome the drawbacks of existing designs that require special fixtures for different workpieces as well as requiring additional equipment. Moreover, the fiducials such as standard balls can also calibrate the measuring systems. Once the fiducial-aided positioning system is established, there is no need for any manual operation to align the workpiece on the machine tool since the fiducials can provide the coordinate information.

The key requirement of the design is the stability of the artefact geometry in the measuring process. Thermal sensitivity due to working temperature and elastic deformation under different gravitational directions are considered as the main factors which should be minimized. In order to limit the thermal expansion and deflection, the ball is made of  $\text{Si}_3\text{N}_4$ .

The fixture and the rods are made of steel. Moreover, some short stems made of steel are used to add to the height of the ball bars to control the deformation. A thermally controlled environment is always necessary in the current experiments. As for the gravitational effect, it can be calibrated on a CMM by rotating the fixture to change the direction of gravity in the process of calibration of the positions of the fiducials, and the details are shown in the following section.

Figure 1 shows an example of the designed system consisting of five fiducials ( $N = 5$ ) mounted on a square fixture on a five-axis fly-cutting raster milling machine tool. Five fiducials (standard spheres) were designed to surround the workpiece in the 3D artefact. The heights of the sphere were 20, 25 and 35 mm, and the distribution of these fiducials is also shown in Figure 2.

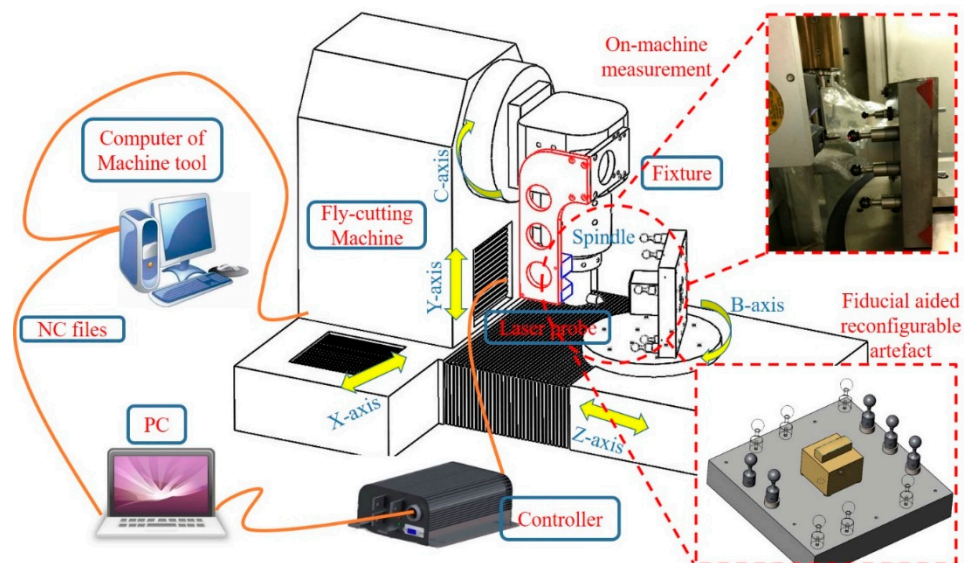


**Figure 1.** A schematic diagram of the fiducial-aided reconfigurable artefact mounted on the B-axis of a five-axis ultra-precision machine tool.

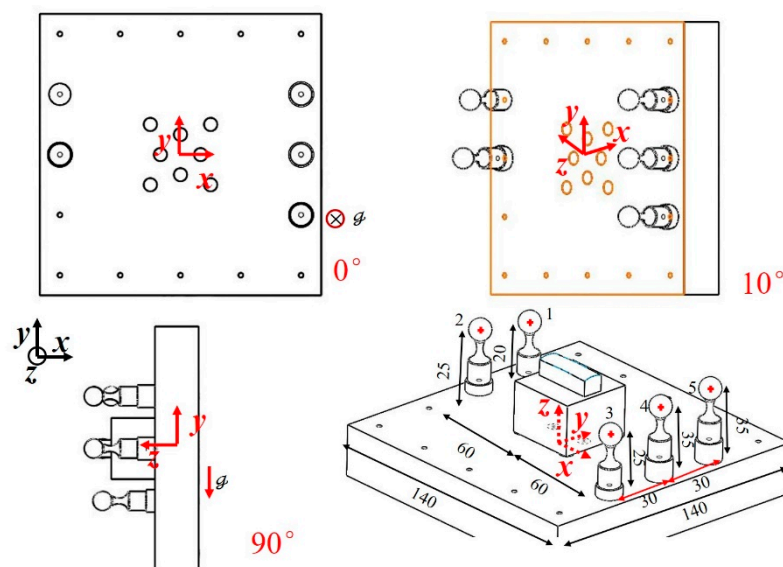


**Figure 2.** The five fiducials-aided 3D artefact measured in different positions.

## 2.2. Gravity Effect on the 3D Artefact

In order to quantify the deviation resulting from gravity ( $\{ \}$ ), three expected positions are measured as shown in Figure 2. One position is the horizontal position (H) meaning

that the mounted ball bar plane of the fixture is parallel to the horizontal plane which is used as a reference position for the  $0^\circ$  position. The second position is the vertical position (V) that is perpendicular to the horizontal plane as the  $90^\circ$  position. The third position is the  $10^\circ$  position (O) from the horizontal position. The units of measurement of the artefact are mm.

The deviations of the two positions including the three dimensions are given by the following equations:

$$\begin{aligned}\Delta x_{i,KH} &= \bar{x}_{i,K} - \bar{x}_{i,H}, \Delta \bar{x}_{KH} = \frac{1}{N} \sum_{i=1}^N |\Delta x_{i,KH}| \\ \Delta y_{i,KH} &= \bar{y}_{i,K} - \bar{y}_{i,H}, \Delta \bar{y}_{KH} = \frac{1}{N} \sum_{i=1}^N |\Delta y_{i,KH}| \\ \Delta z_{i,KH} &= \bar{z}_{i,K} - \bar{z}_{i,H}, \Delta \bar{z}_{KH} = \frac{1}{N} \sum_{i=1}^N |\Delta z_{i,KH}| \\ K &= V, O; i = 1, 2 \dots N\end{aligned}\quad (1)$$

$$\begin{aligned}\Delta d_{i,(x,y,z),KH} &= \sqrt{(\Delta x_{i,KH})^2 + (\Delta y_{i,KH})^2 + (\Delta z_{i,KH})^2} \\ \Delta \bar{d}_{(x,y,z),KH} &= \frac{1}{N} \sum_{i=1}^N \Delta d_{i,(x,y,z),KH}\end{aligned}\quad (2)$$

where  $\bar{x}, \bar{y}, \bar{z}$  are the mean sphere center coordinates with repeating measurement 3 times.  $\Delta d_{i,(x,y,z),KH}$  is the total position variation of the  $i$ th sphere. The effect of gravity is measured, and discussed in Section 3.1.

### 2.3. Probing Fiducials with the On-Machine Measurement System

In this study, a five-axis ultra-precision machine tool incorporated with the developed on-machine measurement system as shown in Figure 1, is used to evaluate the working volumetric error with the fiducial-aided artefact. The positions of fiducials in the artefact are provided by using the probing system for each re-localization of the artefact. A total of 30 points in a  $6 \text{ mm} \times 6 \text{ mm}$  area are sampled uniformly on one standard sphere to guarantee its center position using the least square method. The calibrated diameter of the spherical fiducial was 9.997 mm. Figure 3 illustrates the probing directions.

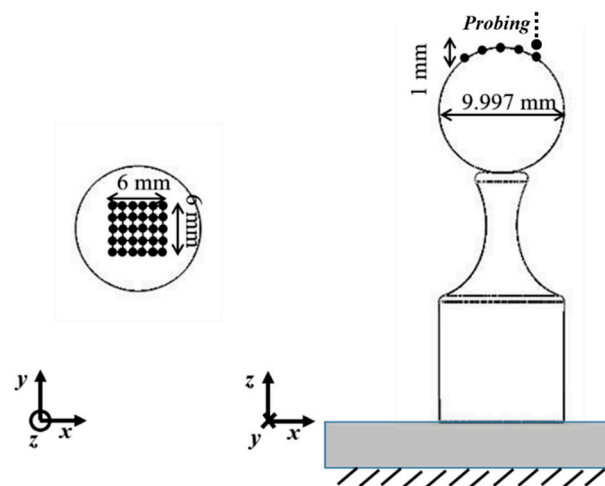


**Figure 3.** Probing points on the standard sphere (left: z view; Right: y view).

In order to reduce the error source caused by the integrated on-machine measurement system, the probe error should be identified before the measuring tasks. The repeatability of measurement of the integrated probing system is evaluated by probing a standard sphere three times. The Cartesian repeatability ranges contributed by the pooled standard deviation are  $0.36 \mu\text{m}$ ,  $0.41 \mu\text{m}$  and  $0.25 \mu\text{m}$  [18], respectively. In addition, the best fitted standard deviations of the sphere center coordinates are  $0.18 \mu\text{m}$ ,  $0.21 \mu\text{m}$  and  $0.24 \mu\text{m}$ , respectively. As for other measurement errors, for instance, the errors of the linear axes and rotary axes, which could affect the measurement results, these are treated as errors caused by the machine tool itself.

#### 2.4. Machine Tool Kinematic Model

The fiducial is used to obtain the probing information containing errors resulting from both the integrated on-machine measurement system and the machine tool itself. The relationship between the tip of the probe and tip of the tool has been established in the previous work of the authors [18]. As mentioned earlier, the repeatability of measurement of the probing system is relatively low at 0.24  $\mu\text{m}$ . It is reasonable to assume that the main contributor of the error sources is the machine tool. As a result, the integrated error effect can be synthesized to find the difference between the actual position and probing position of each fiducial in the working volume. It is not necessary to measure and model all the errors separately. More attention should be focused on the synthesized influence of the measurement task. In the present work, the position errors of the fiducials are mainly considered. The ultra-precision raster milling machine tool has a wBZfXYCt topology as shown in Figure 4.

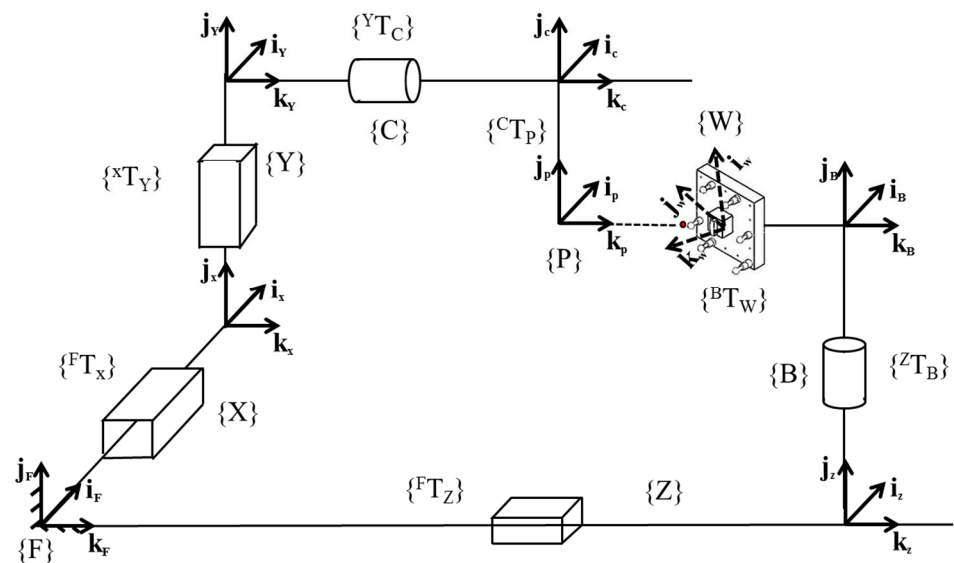


**Figure 4.** Topological construction of the five-axis ultra-precision fly-cutting machine tool.

The homogenous transformation matrix described in Equation (3) is a powerful approach to connect the positions of the fiducials in different coordinates and each single error can be synthesized as a volumetric error.

$${}^jT_i = \begin{bmatrix} {}^jR_i & {}^jm_i \\ 0_{1 \times 3} & 1 \end{bmatrix} \quad (3)$$

${}^jT_i$  is a  $4 \times 4$  homogenous transformation matrix which describes the coordinate transformation from the coordinate frame  $i$  to coordinate frame  $j$ .  ${}^jR_i$  and  ${}^jm_i$  stand for the rotation matrix ( $3 \times 3$ ) and the translation column vector ( $3 \times 1$ ), respectively.

The workpiece and tool branches of the machine tool are determined as follows:

$${}^FT_p = {}^FT_X \cdot {}^XT_Y \cdot {}^YT_C \cdot {}^CT_P \quad (4)$$

$${}^FT_w = {}^FT_Z \cdot {}^ZT_B \cdot {}^BT_w \quad (5)$$

with the four-tool branch sub-matrices which are shown as follows:

$${}^FT_X = \begin{bmatrix} I_{3 \times 3} & x \\ 0_{1 \times 3} & 1 \end{bmatrix} \quad (6)$$

$${}^X T_Y = \begin{bmatrix} 0 \\ I_{3 \times 3} & y \\ 0 \\ 0_{1 \times 3} & 1 \end{bmatrix} \quad (7)$$

$${}^Y T_C = \begin{bmatrix} 0 \\ R_C & 0 \\ 0 \\ 0_{1 \times 3} & 1 \end{bmatrix} \quad R_C = \begin{bmatrix} \cos c & -\sin c & 0 \\ \sin c & \cos c & 0 \\ 0 & 0 & 1 \end{bmatrix} \quad (8)$$

$${}^C T_P = \begin{bmatrix} p_x + \Delta_{px} \\ I_{3 \times 3} & p_y + \Delta_{py} \\ p_z + \Delta_{pz} \\ 0_{1 \times 3} & 1 \end{bmatrix} \quad (9)$$

$${}^F T_P = \begin{bmatrix} x + R_C(p_x + \Delta_{px}) \\ R_C & y + R_C(p_y + \Delta_{py}) \\ R_C(p_z + \Delta_{pz}) \\ 0_{1 \times 3} & 1 \end{bmatrix} \quad (10)$$

The three-workpiece branch sub-matrices are given as follows:

$${}^F T_Z = \begin{bmatrix} 0 \\ I_{3 \times 3} & 0 \\ z \\ 0_{1 \times 3} & 1 \end{bmatrix} \quad (11)$$

$${}^Z T_B = \begin{bmatrix} 0 \\ R_B & 0 \\ 0 \\ 0_{1 \times 3} & 1 \end{bmatrix} \quad R_B = \begin{bmatrix} \cos b & 0 & \sin b \\ 0 & 1 & 0 \\ -\sin b & 0 & \cos b \end{bmatrix} \quad (12)$$

$${}^B T_w = \begin{bmatrix} w_{i,x} + \Delta_{wix} \\ R_w & w_{i,y} + \Delta_{wiy} \\ w_{i,z} + \Delta_{wiz} \\ 0_{1 \times 3} & 1 \end{bmatrix} \quad (13)$$

$${}^F T_w = \begin{bmatrix} R_B(w_{i,x} + \Delta_{wix}) \\ R_B & R_B(w_{i,y} + \Delta_{wiy}) \\ z + R_B(w_{i,z} + \Delta_{wiz}) \\ 0_{1 \times 3} & 1 \end{bmatrix} \quad (14)$$

where  $x$ ,  $y$ ,  $z$ ,  $b$  and  $c$  are the machine axes positions for each fiducial.  $p_x$ ,  $p_y$  and  $p_z$  are the probe center coordinates and  $\Delta_{px}$ ,  $\Delta_{py}$  and  $\Delta_{pz}$  are the setup errors of the probe.  $(w_{i,x}, w_{i,y}, w_{i,z})$  is the position of the  $i$ th fiducials relative to the last axis (B-axis) and  $\Delta_{wix}$ ,  $\Delta_{wiy}$ ,  $\Delta_{wiz}$  are the fiducial  $i$ 's setup errors.  $R_w$  is the rotation matrix and it is usually given as follows in most studies.

$$R_w = I_{3 \times 3} \quad (15)$$

Since there is no need to rotate the spindle in the probing process, the errors resulting from spindle are not included in the above equation model. It is noted that many commercial multi-axis machine tools are not equipped with an on-machine probing system, which means that the developed on-machine probe may have a different coordinate frame from that of the tool tip. Although the established fiducial-aided geometry is likely to minimize the impact of the error source in the measuring procedure, the transformation relationship has to be established before the actual machining process.



The deviation between the probe tip center and the  $i$ th fiducial  $\delta_i$  is described as:

$$\delta_i - \begin{bmatrix} x \\ y \\ -z \end{bmatrix} - R_C \begin{bmatrix} p_x \\ p_y \\ p_z \end{bmatrix} + R_B \begin{bmatrix} w_{i,x} \\ w_{i,y} \\ w_{i,z} \end{bmatrix} = R_C \begin{bmatrix} \Delta_{px} \\ \Delta_{py} \\ \Delta_{pz} \end{bmatrix} - R_B \begin{bmatrix} \Delta_{wix} \\ \Delta_{wiy} \\ \Delta_{wiz} \end{bmatrix} \quad (16)$$

Assuming that the nominal values of the probe tips and fiducials have been estimated, all the error parameters can be treated as per the following linear equation:

$$\Delta\delta = J\Delta E \quad (17)$$

where  $\Delta\delta$  is the deviation between the probe and the fiducials' positions,  $J$  is the Jacobian matrix, and  $\Delta E$  is the error vector including the probe and all the fiducials:

$$\Delta E = [\Delta_{px}, \Delta_{py}, \Delta_{pz}, \Delta_{wix}, \Delta_{wiy}, \Delta_{wiz} \cdots \Delta_{wnx}, \Delta_{wny}, \Delta_{wnz}] \quad (18)$$

$$J = \begin{bmatrix} R_C & -R_B & 0_{3 \times 3} & \cdots & 0_{3 \times 3} \\ R_C & 0_{3 \times 3} & -R_B & \cdots & 0_{3 \times 3} \\ \vdots & \vdots & \vdots & \ddots & \vdots \\ I_{3 \times 3} & 0_{3 \times 3} & 0_{3 \times 3} & \cdots & -R_B \end{bmatrix} \quad (19)$$

The measuring results obtained from the probe and the calibrated artefact geometry are used to access the error parameters using the following system:

$$\Delta F = J\Delta E \quad (20)$$

where  $\Delta F$  denotes the difference between the on-machine measurement results and the calculated positions.

As a result, the volumetric errors in this study can be estimated by comparing the calibrated centers of the fiducials with the calculated centers of the spheres using the above mathematical model.

### 3. Experiments and Discussions

#### 3.1. Measurement of the Gravity Effect

For the five-axis machine tool, the artefact may be mounted in different orientations so that the orientation of the local gravity of the artefact may alter relative to global gravity. As a result, three positions are measured. The position deviations are summarized using the differences between the two tilt positions ( $10^\circ$ ,  $90^\circ$ ) and the horizontal position ( $0^\circ$ ). A multi-sensor coordinate measuring machine (CMM) (Werth Videocheck from Gießen, Germany) was used (a Renishaw trigger probe TP200) to measure the positions of the fiducials. The measurement uncertainty of this machine is  $u = 0.25 + L/300 \mu\text{m}$ .

As shown in Figure 5, the position variations go up when the angle of the artefact increases from the horizontal orientation. Position deviations are mainly below  $1 \mu\text{m}$  in all directions but for fiducials whose heights were more than  $25 \text{ mm}$ ; they could be many to a few micrometers when the artefact is rotated into the vertical position. It is noted that the position deviation in the  $z$  direction (global coordinate frame in Figure 2) seems to be sensitive to the artefact's rotation. This is because the component which is used to connect the fiducials to the fixture has a deformation. The longer the component is, the more obvious the gravitational deformation is. The largest deviation reaches  $\Delta d_{5,VH} = 2.9 \mu\text{m}$  and  $\Delta z_{5,VH} = 2.1 \mu\text{m}$  in synthesis direction and only the  $z$  direction, respectively, when the gravitational orientation is changed from  $-z$  to  $-y$  for the local coordinate frame.

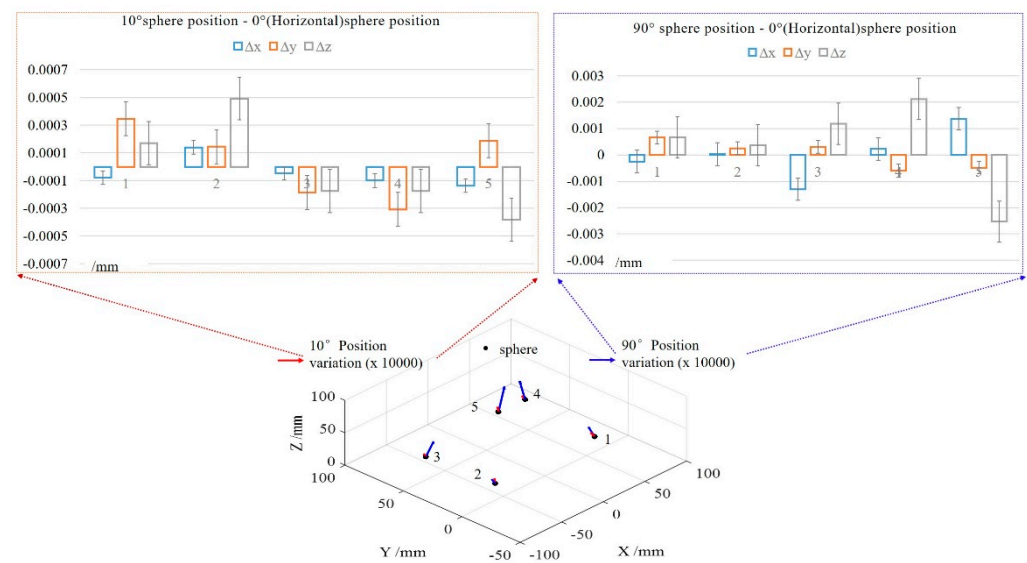


**Figure 5.** Position deviations of the fiducials when changing the artefact from a horizontal to a 10-degree (O-H) position and into a vertical orientation (V-H). The error vectors are multiplied by 10,000 in the bottom plot. The top two graphs are position deviations in three directions with their uncertainties.

In this study, the effect caused by gravitational deformation still needed to be considered although it is as small as a few micrometers. As shown in Figure 5, the results indicate that there are two facts which can be considered to reduce the effect. It is necessary to optimize the length of the connection component to be as short as possible with consideration of the working volume. In other words, it is helpful to add stiffness to the artefact. The other is that the artefact can be measured in a stable position in each measurement. For example, it is better to carry out the metrology in a horizontal position ( $0^\circ$ ) as shown in Figure 2 in every measurement instrument. In this case, the measurement repeatability should be guaranteed in a particular position. Taking these two points into consideration, the height of each fiducial (z value as shown in Figures 2 and 3) is controlled within 25 mm and the artefact was clamped in a vertical position in every measurement process and instrument; the raster milling machine tool and the coordinate measuring machine are used in this case. The deformations due to weight are finally controlled to an acceptable level, and the largest deformations are  $\Delta \bar{z} \leq 0.3 \mu\text{m}$  and  $\Delta \bar{d}_{(x,y,z)} \leq 0.45 \mu\text{m}$ , respectively.

### 3.2. On-Machine Measurement

To determine the volumetric error of the five-axis horizontal machine with wBZfXYCt topology as shown in Figure 1, a five-standard sphere artefact is purposely designed as shown in Figure 2 with variation of the height of each fiducial. Each calibrated center position of the fiducial is listed in Table 1.

**Table 1.** Centre positions of the fiducials.

Ball	X (mm)	Y (mm)	Z (mm)
1	59.31108	−0.25560	14.99509
2	−58.74790	0.864597	14.29131
3	−59.13960	59.79868	19.31120
4	59.49720	59.29094	24.40756
5	28.48006	59.94329	24.75141

In order to reduce the thermal effect on the fixture, the designed artefact is transformed and kept in a thermally controlled environment and measured by the on-machine probing system. According to the on-machine measurement system, the artefact was clamped in



the vertical position on the B-axis as shown in Figure 1. A number of tests were carried out by gradually increasing the rotary B- and C-axis in the measurement process. All the fiducials were probed to establish their center coordinates and the positions ( $x$ ,  $y$ ,  $z$ ,  $b$  and  $c$ ) of the corresponding axes were also recorded. Considering the working volume of the measurement and machining conditions, a total of 165 standard sphere centers were measured at the locations of  $b = 0^\circ$ ,  $c = 0^\circ$ ;  $b = 0^\circ$ ,  $c = \pm 5^\circ$ ;  $b = \pm 5^\circ$ ,  $c = 0^\circ$ ;  $b = \pm 10^\circ$ ,  $c = 0^\circ$ ;  $b = \pm 5^\circ$ ,  $c = \pm 5^\circ$  which was repeated three times in about two hours.

As shown in Figure 6, the fiducial center distances in a five-fiducial artefact were compared with the distances in the fiducial-aided CAD (calibrated fiducials and the CAD of the designed surface [18]) by using the cloud point fitting algorithm. The tested positions of the fiducials are determined and transferred into a common frame using the mathematical model. Table 2 shows the compared results including the maximum value ( $r_{\max}$ ) and average values ( $r_{\text{avg}}$ ) for a total of 10 distances in the artefact under different angular positions of the rotary axes. Value  $r$  is defined in Figure 6.

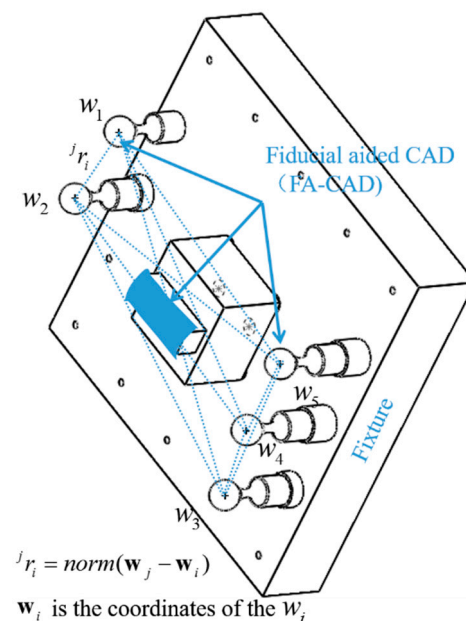


**Figure 6.** Geometrical definition of a five-standard sphere artefact.

**Table 2.** Error of fiducial distances compared with the datasets in FACAD when using the measured results and mathematic model under different rotation angles of axes.

Position of the Rotary Axes		① Measured ( $\mu\text{m}$ )		② Mathematic Model ( $\mu\text{m}$ )		①–② ( $\mu\text{m}$ )	
<b>b</b>	<b>c</b>	$r_{\max}$	$r_{\text{avg}}$	$r_{\max}$	$r_{\text{avg}}$	$r_{\max}$	$r_{\text{avg}}$
$0^\circ$	$0^\circ$	0.9	0.4	0.8	0.4	0.1	0.0
$0^\circ$	$5^\circ$	5.5	1.3	5.1	1.2	0.4	0.1
$0^\circ$	$-5^\circ$	5.4	1.1	5.3	1.1	0.1	0.0
$5^\circ$	$0^\circ$	1.1	0.6	0.8	0.4	0.3	0.2
$5^\circ$	$5^\circ$	5.6	1.6	5.5	1.5	0.1	0.1
$5^\circ$	$-5^\circ$	5.7	1.4	5.4	1.5	0.3	−0.1
$10^\circ$	$0^\circ$	1.6	0.6	1.3	0.8	0.3	−0.2
$10^\circ$	$5^\circ$	6.8	2.3	6.2	2.0	0.6	0.3
$10^\circ$	$-5^\circ$	6.4	2.2	6.1	1.8	0.3	0.4

Notes: ① Measured value minus that in FACAD; ② Mathematical model value minus that in FACAD.

As shown in Table 2, in the measured columns, it is clear that the deviations are very small—0.9  $\mu\text{m}$  at most when the measuring process is carried out with no rotation of the axes—which means that only three linear axes are used to perform the measurement. With the B-axis set to  $0^\circ$ , the error increased with increasing angular positions of the C-axis and

reached  $6.5\ \mu\text{m}$ . In this case, the volumetric errors resulting from the linear axes and errors from the C-axis are integrated into a fiducial when changing the position of the C-axis. It is interesting to note that the error only reaches  $6.8\ \mu\text{m}$  when both angular positions of the rotary axes are combined. The results in the mathematical model suggest that the errors are slightly smaller than those in the measured datasets. This is due to the existing setup errors of the integrated measuring system.

In addition, the residuals of the fiducials after best fitting to those calibrated in the CMM are illustrated in Table 3. The results show that the maximum residual of the sphere diameters is up to  $1\ \mu\text{m}$ .

**Table 3.** The sphere diameter deviations.

	x ( $\mu\text{m}$ )	y ( $\mu\text{m}$ )	z ( $\mu\text{m}$ )
Sphere 1	0.4	0.9	0.2
Sphere 2	0.5	0.8	0.4
Sphere 3	0.7	0.8	0.3
Sphere 4	0.7	1.0	0.3
Sphere 5	0.6	0.7	0.2

### 3.3. Discussion of the Volumetric Errors

As defined in Section 2.4, the volumetric errors can be presented as the differences between the modeled and calibrated positions of the fiducials. According to the measured results shown in Table 2, an easy-to-digest figure as shown in Figure 7 is presented with vector representations of the errors at the positions in the coordinate of machine tool. The length of the arrow represents the value of the error, and the direction of the arrow is decided by the integrated value of three coordinates. The error vectors are multiplied by 10,000. The mean of the volumetric errors is  $4.5\ \mu\text{m}$ .

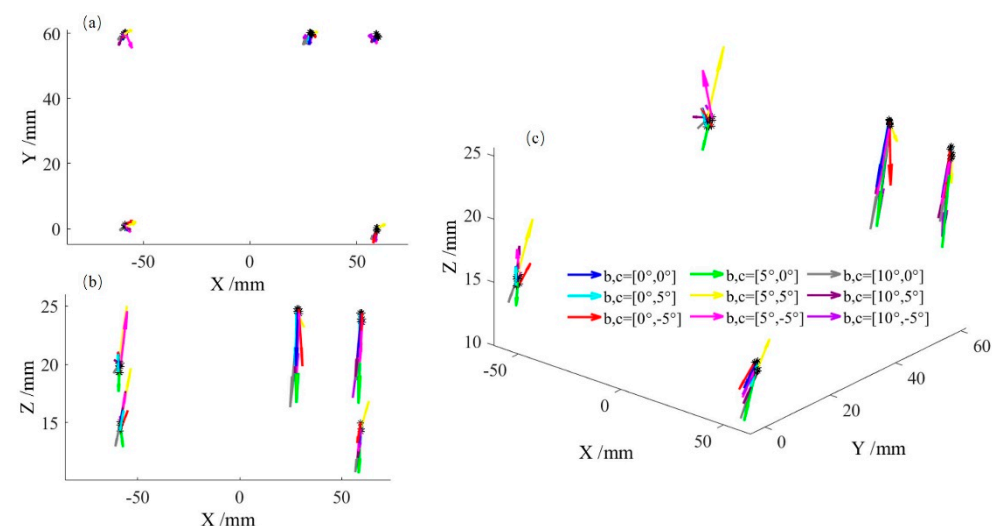


**Figure 7.** Distribution of the volumetric errors of the multi-axis machine tool occupied by the workpiece at nine locations by rotating the b and c axes: (a) xy view, (b) xz view, (c) 3D view, the errors are multiplied by 10,000.

A total of nine locations of the artefact are measured and three measurement tasks are performed to enhance the measurement accuracy. Figure 7 gives the detailed information of the second of the three measurement tasks. The maximum standard deviation between the datasets at different positions is  $0.8\ \mu\text{m}$ . It is clear that the large BC offset has a large effect on the volumetric error of the ultra-precision machine tool.

In the current study, the standard ball served as a fiducial and was mainly used in the experiments. Not only is it easy to be measured by the developed on-machine measurement

system from multiple locations, but also the cost of the standard ball bought from the market is low. Furthermore, it may transfer the accuracy of an off-machine measurement system to the working machine tool. In our future research, the performances of other types of fiducials and artefacts may be investigated.

#### 4. Conclusions

In this paper, a fiducial-aided configurable artefact is proposed to evaluate the volumetric error of a five-axis ultra-precision raster milling machine tool with an on-machine probing system. The 3D artefact allows flexibility in the number and position of the fiducials according to the characteristics of the machine tool. A mathematical model is established to obtain the volumetric errors from the probing results. Measurement repeatability of the on-machine probing system is estimated at 0.24  $\mu\text{m}$ . A detailed analysis of the effect of deflection due to gravity by tilting the artefact from a horizontal into a vertical orientation indicates that the stable orientation of the artefact and the length of connecting fiducial components which is as short as 25 mm can further reduce the errors of the artefact to lower than 0.8  $\mu\text{m}$ . Experiments are carried out using a 3D artefact consisting of five standard spheres on a five-axis machine tool with wBZfXYCt topology. The distance method is employed in the estimation of the volumetric error by comparing the measured results and calculated values with those in the generated FA-CAD on a high-precision CMM. When using the three linear axes, the maximum error is only 0.9  $\mu\text{m}$ . This value slightly increases to 1.6  $\mu\text{m}$  when the rotary B-axis is used. However, when both items of information of the rotary axes are associated, the worst error could sharply increase to 6.8  $\mu\text{m}$ . Compared with the values obtained in the mathematical model, it is found that the setup errors make little contribution to the volumetric error in the measuring process. The results show that the proposed 3D artefact possesses the ability to provide volumetric error occupied by the workpiece when a manufacturing process is carried out.

**Author Contributions:** S.W. and C.C. conceived and designed the methodology and experiments; S.W. and L.K. completed the modeling and simulation. S.W. performed the experiments; S.W. wrote the draft technical content of the manuscript while C.C. reviewed and revised the detailed content of the manuscript. All authors have read and agreed to the published version of the manuscript.

**Funding:** This research was funded by National Key R&D Programs of China grant number 2017YFA0701200, International Partnership Scheme of the Bureau of the International Scientific Cooperation of the Chinese Academy of Sciences grant number Project No.: 181722KYSB20180015. And The APC was funded by the Research Grants Council of the Government of the Hong Kong Special Administrative Region, China (Project No.: 15202814).

**Acknowledgments:** The work described in this paper was supported by National Key R&D Programs of China (2017YFA0701200). The authors would also like to express their sincere thanks to the funding support from the International Partnership Scheme of the Bureau of the International Scientific Cooperation of the Chinese Academy of Sciences (Project No.: 181722KYSB20180015) and the Research Grants Council of the Government of the Hong Kong Special Administrative Region, China (Project No.: 15202814).

**Conflicts of Interest:** The authors declare that there is no conflict of interest.

#### References

1. Liebrich, T.; Bringmann, B.; Knapp, W. Calibration of a 3D-ball plate. *Precis. Eng.* **2009**, *33*, 1–6. [\[CrossRef\]](#)
2. Zhu, S.; Ding, G.; Qin, S.; Lei, J.; Zhuang, L.; Yan, K. Integrated geometric error modeling, identification and compensation of CNC machine tools. *Int. J. Mach. Tools Manuf.* **2012**, *52*, 24–29. [\[CrossRef\]](#)
3. ISO230-1; Test Code for Machine Tools Part 1: Geometric Accuracy of Machines Operating under No-Load or Quasi-Static Conditions. ISO: Geneva, Switzerland, 2012.
4. Tian, W.; Gao, W.; Zhang, D.; Huang, T. A general approach for error modeling of machine tools. *Int. J. Mach. Tools Manuf.* **2014**, *79*, 17–23. [\[CrossRef\]](#)
5. Okafor, A.C.; Ertekin, Y.M. Derivation of machine tool error models and error compensation procedure for three axes vertical machining center using rigid body kinematics. *Int. J. Mach. Tools Manuf.* **2000**, *40*, 1199–1213. [\[CrossRef\]](#)

6. Jha, B.K.; Kumar, A. Analysis of geometric errors associated with five-axis machining centre in improving the quality of cam profile. *Int. J. Mach. Tools Manuf.* **2003**, *43*, 629–636. [[CrossRef](#)]
7. Yang, J.; Altintas, Y. Generalized kinematics of five-axis serial machines with non-singular tool path generation. *Int. J. Mach. Tools Manuf.* **2013**, *75*, 119–132. [[CrossRef](#)]
8. Xiang, S.; Altintas, Y. Modeling and compensation of volumetric errors for five-axis machine tools. *Int. J. Mach. Tools Manuf.* **2016**, *101*, 65–78. [[CrossRef](#)]
9. Ibaraki, S.; Knapp, W. Indirect Measurement of Volumetric Accuracy for Three-Axis and Five-Axis Machine Tools: A Review. *Int. J. Autom. Technol.* **2012**, *6*, 110–124. [[CrossRef](#)]
10. Wan, A.; Song, L.; Xu, J.; Liu, S.; Chen, K. Calibration and compensation of machine tool volumetric error using a laser tracker. *Int. J. Mach. Tools Manuf.* **2018**, *124*, 126. [[CrossRef](#)]
11. Aguado, S.; Samper, D.; Santolaria, J.; Aguilar, J.J. Identification strategy of error parameter in volumetric error compensation of machine tool based on laser tracker measurements. *Int. J. Mach. Tools Manuf.* **2012**, *53*, 160. [[CrossRef](#)]
12. Tsutsumi, M.; Saito, A. Identification and compensation of systematic deviations particular to 5-axis machining centers. *Int. J. Mach. Tools Manuf.* **2003**, *43*, 771–780. [[CrossRef](#)]
13. Zargarbashi, S.H.H.; Mayer, J.R.R. Assessment of machine tool trunnion axis motion error, using magnetic double ball bar. *Int. J. Mach. Tools Manuf.* **2006**, *46*, 1823–1834. [[CrossRef](#)]
14. Erkan, T.; Mayer, J.R.R.; Dupont, Y. Volumetric distortion assessment of a five-axis machine by probing a 3D reconfigurable uncalibrated master ball artefact. *Precis. Eng.* **2011**, *35*, 116–125. [[CrossRef](#)]
15. Bringmann, B.; Küng, A.; Knapp, W.A. Measuring Artefact for true 3D Machine Testing and Calibration. *CIRP Ann. Manuf. Technol.* **2005**, *54*, 471–474. [[CrossRef](#)]
16. Mayer, J.R.R. Five-axis machine tool calibration by probing a scale enriched reconfigurable uncalibrated master balls artefact. *CIRP Ann. Manuf. Technol.* **2012**, *61*, 515–518. [[CrossRef](#)]
17. Mayer, J.R.R.; Hashemiboroujeni, H. A ball dome artefact for coordinate metrology performance evaluation of a five axis machine tool. *CIRP Ann. Manuf. Technol.* **2017**, *66*, 479–482. [[CrossRef](#)]
18. Wang, S.; Cheung, C.; Ren, M.; Liu, M. Fiducial-aided on-machine positioning method for precision manufacturing of optical freeform surfaces. *Opt. Express* **2018**, *26*, 18928–18943. [[CrossRef](#)] [[PubMed](#)]